

Thermal Imaging of laser-tissue interaction using color Schlieren techniques quantified by ray-tracing simulation

*Rudolf M. Verdaasdonk, Rogier Lodder,
Christiaan F.P. van Swol and Matthijs C. Grimbergen*

Dept. Clinical Physics and Laser Center, University Hospital, Utrecht,
The Netherlands NL 3508 GA

ABSTRACT

In various studies the use of a color Schlieren technique to visualize the dynamic thermal effects of lasers in an aqueous environment has proven to be very useful. Besides for the research, this setup but has also proven to be very successful for education and demonstration purposes. This 'pseudo thermal imaging' technique has also been applied to study the behavior of diathermia devices and ultrasound resectors used in surgery. Since, the images reflect gradients in refractive index induced by thermal gradients, they can not simply be converted and interpreted as thermal images. In order to understand the pathway of light through thermal gradients, a ray-trace program was developed.

The program is capable of visualizing the path of light rays through simulated thermal gradients as well as generating an image, which can be compared with the 'real' images from the color Schlieren setup. For calibration, the program was successfully tested on well defined optical configurations such as spherical and index-gradient lenses. Images calculated using data from a temperature profile measured with a small thermocouple appeared to be almost similar to the actual Schlieren image. Matching the calculated and actual image was possible by either assuming a minimal error in the temperature measurements or in the temperature dependence of the refractive index.

The ray-trace program has been a helpful tool to quantify the absolute temperatures in color images from simple geometries. Expanding the code might enable the quantification of more complex temperature gradients. Such information is valuable for the clinical application of energy source such as lasers.

1. INTRODUCTION

For several years we have been using a color schlieren setup to study the thermo dynamical processes involved during energy deposition in physiological media¹. This method enables the visualization of small changes of refractive index induced by a temperature gradient in a artificial tissue model resulting in a pseudo thermal image. This setup has successfully been applied to extend our knowledge of interaction of various energy sources like lasers^{2,3,4} and electro surgery generators⁵ with biological tissues. The real-time thermo dynamic images obtained are useful for qualitative and comparative studies and educational purposes. However, it is not possible to assign absolute temperatures to colored areas in images. During the last years, we have attempted to calibrate the colors in the images⁶. If the temperature gradient is of a simple one-dimensional geometry, a direct relation between colors and temperature can be obtained. For more complex geometries (two-dimensional), it becomes difficult to deduce absolute temperature from the images.

The interpretation of the images could be improved, understanding the way the images are 'created'. By following the path of a ray step by step through a temperature gradient, it is possible to observe which factors contribute most to the resultant color and position of a ray when it reaches the image plain. For this purpose, a ray trace program was developed to simulate the color images obtained using our color Schlieren technique and compare them with actual images of temperature gradients.

Correspondence: r.m.verdaasdonk@id.azu.nl; <http://www.urolog.nl/lasercenter>;
tel. 31-30-2507302; fax. 31-30-2542002

2. COLOR SCHLIEREN OPTICS

In Figure 1 the optical setup for the study of thermodynamic processes during heat application in tissue is illustrated. The setup is based on Schlieren techniques^{7,8}.

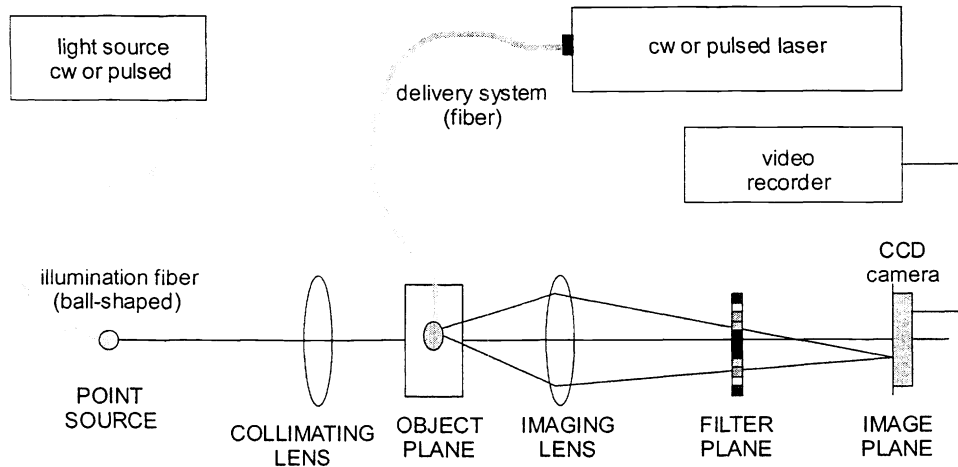


Figure 1: Schlieren setup to study laser tissue-interaction

A continuous or pulsed white light source is coupled into a ball-shaped fiber. The light emitted from the fiber is focused due to the spherical fiber end and divergences subsequently. The focal point of a collimating lens coincides with the focus of the fiber. The diameter of the lens is matched with the divergence of the beam so all light is collimated. A rectangular tank filled with water is positioned between the collimator and imaging lens, the 'object' plane. The walls are perpendicular to the parallel beam to prevent any optical distortion due to refraction. Within this tank, conditions are created to study laser tissue interaction. The imaging lens will focus the parallel beam in its focal point on the optical axis. However, rays can be deflected due to variations in the refraction index or irregularities in the medium in the object plane induced by local stresses or temperature gradients. These rays will cross the focal plane at a particular distance d from the optical axis (Figure 2).

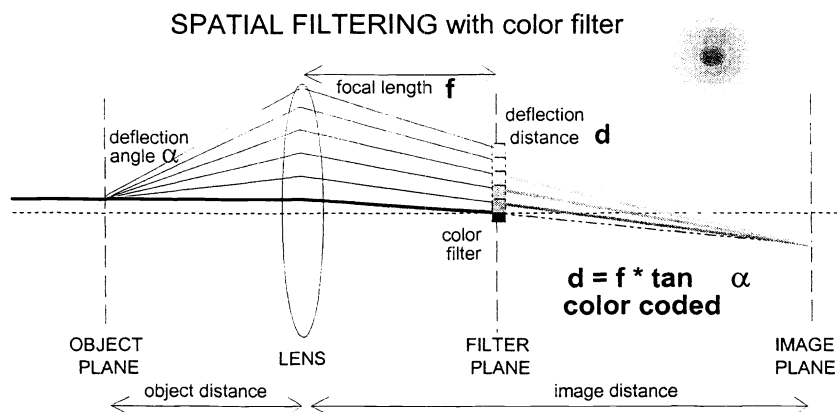


Figure 2: Scheme of spatial filtering using a color filter

The non distorted rays will be focused on the optical axis. By inserting a mask or a filter in the focal plane of the imaging lens, it is possible to block out the non-deflected rays, preventing them to reach the image plane. This process of modifying the object information in the focal or filter plane is known as spatial filtering. By blocking the rays crossing the optical axis, only refracted and diffracted rays will pass the filter plane and form an image at the image plane. Due to the subtraction of the background light, an enormous contrast enhancement of the image is achieved. Depending on the deflection angle α and

the focal length of the transform lens, a ray will pass the filter plane at a deflection distance d from the optical axis (Figure 2):

$$d = f * \tan \alpha.$$

The information on the degree of deflection can be preserved by color coding the rays coming through the filter plane using a color filter (inset Figure 2). This filter consists of concentric rings of discrete color bands separated by small black rings. The center of the filter is a black dot blocking the background light. Adjacent to the black dot, going away from the center, the colors shift gradually from blue to red. Rays passing the filter plane will be color coded depending on the deflection distance d and will be reconstructed to an image at the image plane. The generated color image will show, position dependent, the degree of deflection in the object plane. From each color, the deflection angle α can be determined which is related to the variation in the refractive index of the medium in the object plane. The color image can be interpreted as a thermal image when the relation between refractive index and temperature gradient is known. The black rings in the filter will result in black lines in the image separating the discrete colors giving an impression of 'isotherms' (Figure 3).

The position of the imaging lens, the filter and the CCD camera are chosen depending on the magnification desired according to the lens formula. The diameter of the filter determines the dynamical range of temperatures that can be visualized. Using a x-y microtranslator, the filter can be optimally aligned on the optical axis. The CCD camera is positioned in the image plane. Additional filters can be used to filter out scattered light from the primary laser wavelength. To obtain microsecond resolution, a video camera with high-speed mode can be used.

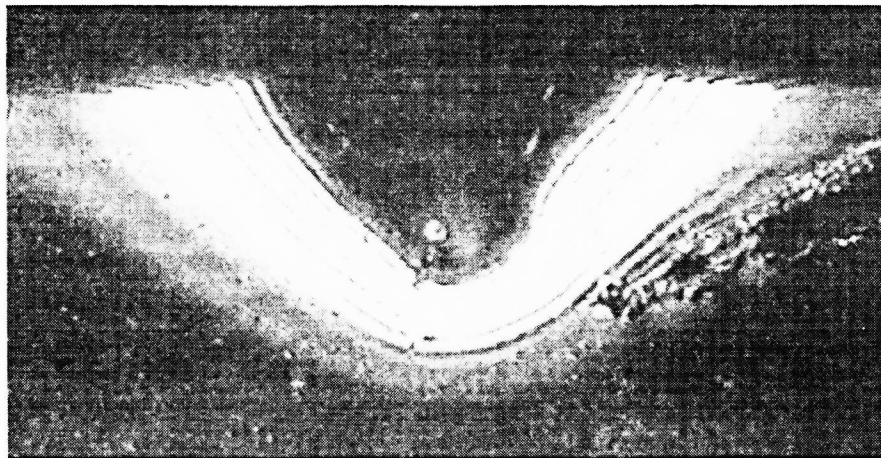


Figure 3: Example of a color coded image showing the thermal zone around an ablation crater during laser irradiation. The black lines can be interpreted as isotherms

3. THE RAY-TRACE PROGRAM

In literature ⁹, it has been shown possible to analytically calculate a ray-trace through a non-homogenous medium. There are however two problems. In order to do the calculation, it is necessary to make assumptions and simplifications. Furthermore, these calculations can only be performed for very basic temperature distributions. Since tracing a ray in a non-uniform medium is essentially an iterative calculation, which can become far too large to evaluate analytically. The only way to do the calculation is by computer, in which case it is called ray-tracing. There are many commercial ray-tracing applications on the market today, but these either put the emphasis on rendering or are expensive and complicated. For this reason, we developed a ray-tracing program that will not only do the ray-tracing but also generate the resulting Schlieren images.

3.1 The ray-trace algorithm

Basically, a ray-trace program performs a simulation of a light ray through a medium. By taking a small ray of length dx , it calculates the refraction of that ray due to any differences in refractive index at the location of the ray. There are three possibilities for the refraction:

1. The refraction is calculated using Snell's law of refraction ¹⁰:

$$n_1 \cdot \sin(\theta_1) = n_2 \cdot \sin(\theta_2)$$

2. The refraction index difference is such that total reflection occurs. In this case, the angle of reflection is equal to the angle of incidence.
3. If there are no differences in refractive index, or if the ray travels parallel to the refractive-index gradient, then the refraction is non-existent

When the new direction is determined, the program then linearly extrapolates the refracted ray for a length of dx to the new position and then starts the process over again using the new ray as the starting point. This is repeated until the ray has reached certain position or length. The advantage of this kind of algorithm is that it's very simple as well as easy to implement. The downside is that it can be a very time-consuming calculation since the accuracy depends on dx . This means that for a high accuracy dx has to be small. However, it also means that more iteration will be needed.

3.2 Mathematics of the ray-tracing algorithm

Figure 4 shows the vectors defined for the calculation in 3D with \vec{a} pointing along the path of the ray, \vec{p} the position of the ray in the medium, \vec{n} the direction of the refractive index gradient, and \vec{a} -new as the refracted ray.

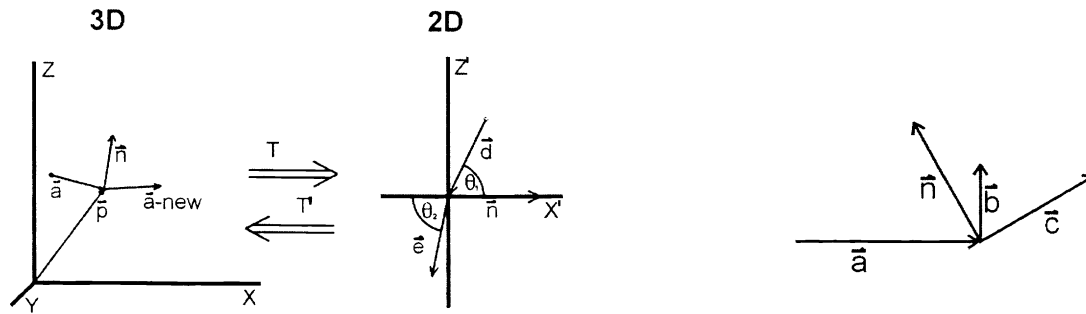


Figure 4: definition of vectors transformed between 3D and 2D systems (left) and a normalized system (right)

The vectors are transformed in such a way that all the relevant vectors lay in one 2D plane, making it possible to apply Snell's law. This transformation T turned \vec{a} into \vec{d} , and another transformation T' turns \vec{e} (the refracted ray) into \vec{a} -new (the new 3D ray)¹¹. The norm of all vectors except \vec{p} is 1. The original coordinate system O is linear transformed by the 3x3 matrix T to O' . The matrix T' performs the transformation of the vectors back from O' to O . The coordinate system in the right in Figure 4 shows the vectors \vec{a} and \vec{n} and two additional vectors \vec{b} and \vec{c} . The vector \vec{n} is the gradient of the refractive index distribution, meaning that it is the normal of the imaginary plane of incidence. The angle between \vec{n} and \vec{a} is the angle of incidence. The three vectors \vec{n} , \vec{b} and \vec{c} are all perpendicular to each other and they are of length 1. This makes them a basis for the new coordinate system called O' . In this coordinate system \vec{a} has no component in the direction of \vec{b} . So if \vec{a} is transformed from O to O' its y-component will be zero. As a result, Snell's law is easy to apply. The resulting refracted ray will also have a zero y-component in this system. By transformation with T' , \vec{a} -new is part of the original 3D system. It follows that T' consists of the components of vectors \vec{n} , \vec{b} and \vec{c} :

$$T' = \begin{pmatrix} n_1 & b_1 & c_1 \\ n_2 & b_2 & c_2 \\ n_3 & b_3 & c_3 \end{pmatrix}$$

The components of T' are calculated in the following way: The vectors \vec{n} and \vec{a} are always in the same plane. Vector \vec{b} is calculated by taking the crossproduct of \vec{a} and \vec{n} . Vector \vec{c} by taking the crossproduct of \vec{n} and \vec{b} . When a crossproduct is calculated, the norm of the resulting vector is not automatically equal to 1, it depending on the angle between the two. Because of this, it is necessary to make every vector of length 1 after performing a crossproduct. From T' , T can be derived.

3.3 The structure of the ray-trace program

The ray-tracing is performed in a pre-determined volume presented in Figure 5 with the relevant dimensions. At the beginning of the program, the dimensions of this volume along with the information of the refractive index gradient are loaded from a data file¹². The iteration is started in the main program for a preset number of rays at different starting positions covering the whole field of view. For each step, at the position of the ray in space, the refractive index gradient is determined in relation to the direction of the ray.

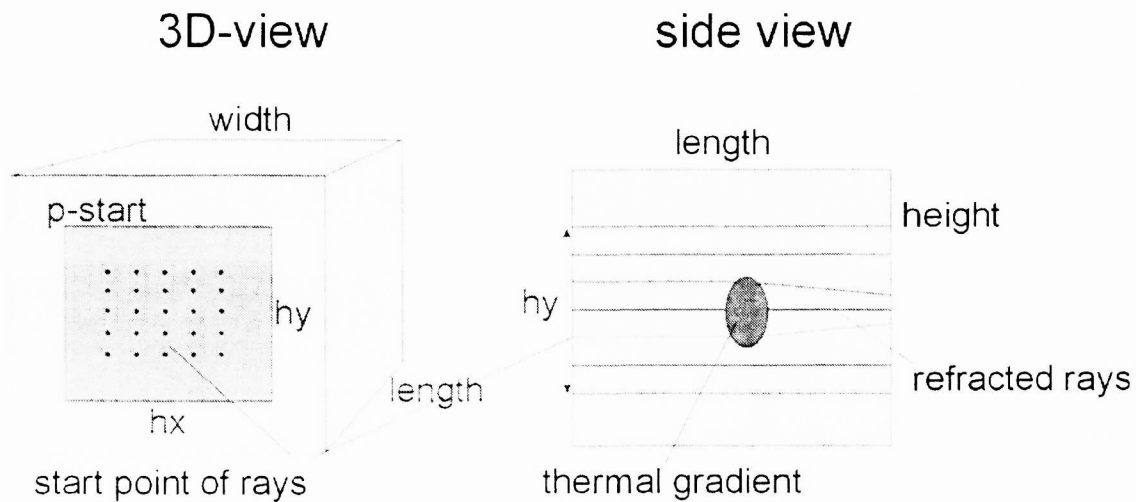


Figure 5: 3-D volume in which the ray-tracing is performed and view from the side

The refractive index gradient is derived from e.g. a spherical or cylindrical temperature distribution. For a cylindrical heat distribution, a typical function would be :

$$T(r) = 20 + 200 \cdot e^{-r \cdot 1.24}$$

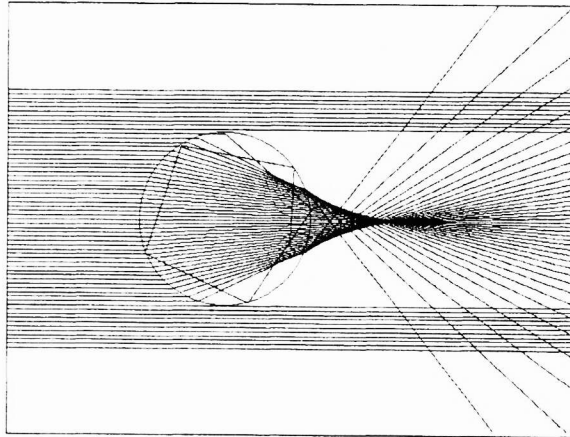
For a particular temperature at the position of the ray, the refractive index is calculated from a sixth-order polynomial fitted on the refractive index of water in relation to temperature¹². Then the vector representing the ray and the vector representing the gradient are transformed in normalized dimensions from 3-D volume to a 2-D plane, where the calculation takes place if the ray is either refracted or reflected. A new position of the ray is calculated for the ray by inverse transformation to the 3-D volume. This process continues until the ray has reached the image plane or 'escapes' from the field of view.

Depending on the direction or angle of the ray in the images plane, a color is assigned to the pixel at the position where the ray entered the image plane. This color is related to the design rainbow filter of this 'virtual' Schlieren setup. The distance from the optical axis where the ray intersects the filter is calculates with $d = \tan(\alpha_{\text{ray}}) \cdot f_{\text{decollimator}}$ (Figure 2). The angle α_{ray} is the angle between the ray and the optical axis. The format of the filter is known to the program, so the color can be determined. Next, the procedure calculates where the ray intersects the CCD of the camera. This is done using the lens formula rather than ray-tracing. Finally, the ray is displayed on the screen and a new ray is started. After all the rays have been traced, the 'schlieren' image is displayed which can be compared with a 'real' image

4. VALIDATION OF THE SCHLIEREN RAY-TRACE PROGRAM

The ray-tracing program is essentially a computer simulation. As such, its results are not exact, meaning that they can not be verified analytically. The only way to ascertain whether the program is functioning properly is to perform some simulations of which the outcome is well known. One check is the tracing of a perfect sphere like a raindrop ($n=1.33$) in air where refraction and internal reflection can be expected.

Figure 6:
Ray-trace result through a
spherical 'raindrop' in air



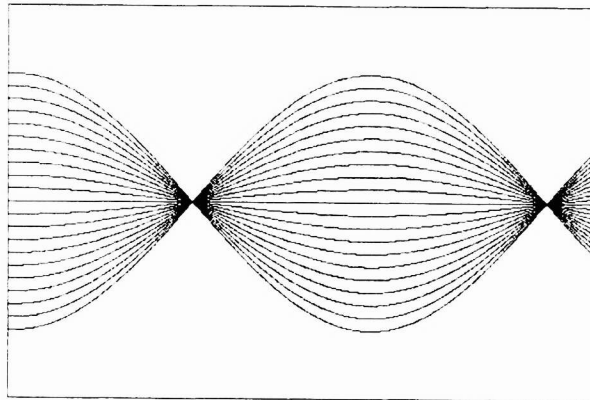
Spherical aberration and total internal reflection are evident in the ray-trace presented in Figure 6. Rays hitting the sphere from a sufficiently small angle will get "trapped" inside the sphere. The program stops any ray after a certain amount of iterations to prevent the well-known infinite loop. However, this example is not challenging since there were only two refractions at the boundary surfaces, while the ray-tracing was performed in small step. The same result could have been obtained by calculating the intersection of the ray with the next boundary surface and only calculating the refraction in that point. Most of the commercial optical programs work this way.

The best test is performed by tracing a selfoc or index gradient lens. In an index gradient-lens, which can be anything from a small cylinder to a rod, the refractive index of the material is a function of the radius:

$$n(r) = n_0 \left(1 - \frac{A}{2} r^2\right)$$

where, n_0 is the refractive index of the center, r is the radius and A is a positive constant. Because of this parabolic index variation, a ray entering the lens at the front surface will follow a sinusoidal path through the lens. A simulation of such lens is presented in Figure 7.

Figure 7:
Ray-trace through an index
gradient lens.



As predicted, the rays travel along the lens in a sinusoidal path. More importantly, they are focussed twice in a perfect focal point.

5. RAY TRACE SIMULATION OF THE COLOR SCHIEREN SETUP

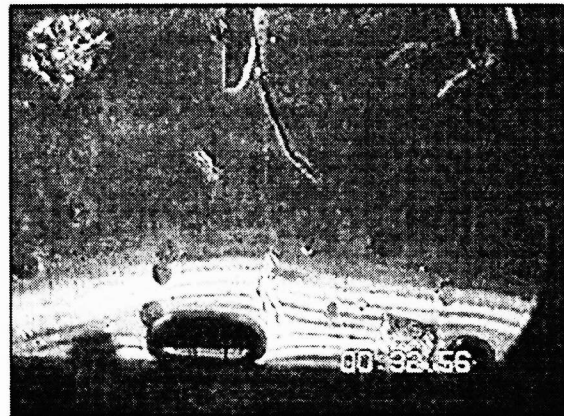
5.1 Validation of the ray-trace program for a temperature gradients

The validation of the program for the color Schlieren setup is performed for a cylinder-symmetric temperature distribution. This distribution can be modeled easily and accurately into a computer program and compared to an actual cylindrical heat distribution visualized with the color Schlieren setup. Other basic temperature distributions, such as plan-parallel or spherical are also possible but are more troublesome to realize.

Before the ray-tracing could be performed, the well defined temperature distribution needed to be determined as input for the program. This distribution also had to be created in reality in the color Schlieren setup for verification of the ray-trace result.

Instead of using a temperature profile calculated from theory where various assumptions had to be made, the temperature profile was determined empirically by actual measurements. Using a 0.05 mm diameter T-type thermocouple, the temperature profile perpendicular to a 2 mm diameter metal rod at a constant temperature of 90 °C was measured. To reduce convection, the cylinder was positioned inside a 90% water containing polyacrylamide gel which is also used as tissue model. The temperature measurement was performed simultaneously with color Schlieren imaging for comparison. Figure 8 shows an image obtained during the measurement. From the image, the position of the thermocouple could be determined with accuracy up to μm .

Figure 8:
Schlieren image during temperature
measurement above a hot cylinder.
The thermocouple is the thin wire
supported by the needle at the top.



The temperature profile obtained during this experiment is presented in Figure 9. Using the curve fit $t(r)=20+115\cdot e^{-0.6r}$ as input in the ray-trace program, the 'Schlieren' image presented in Figure 10 (right) was generated. For orientation, the right side image can be compared best to Figure 5.

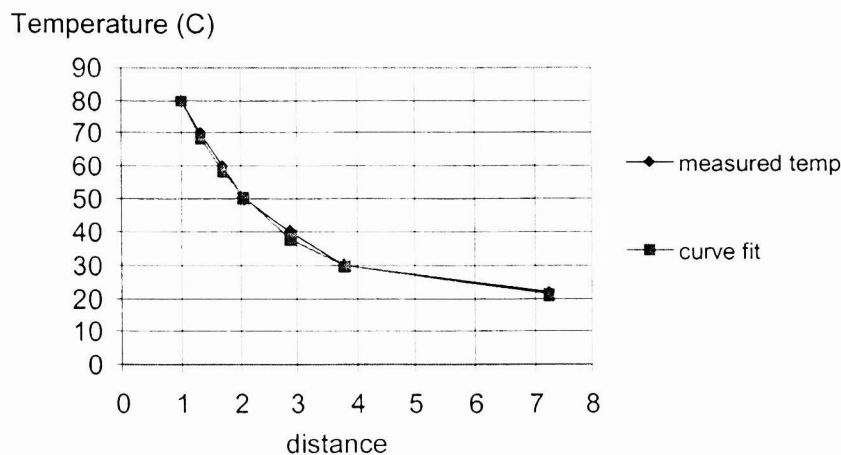


Figure 9: Temperature profile measured perpendicular to a hot cylinder surface

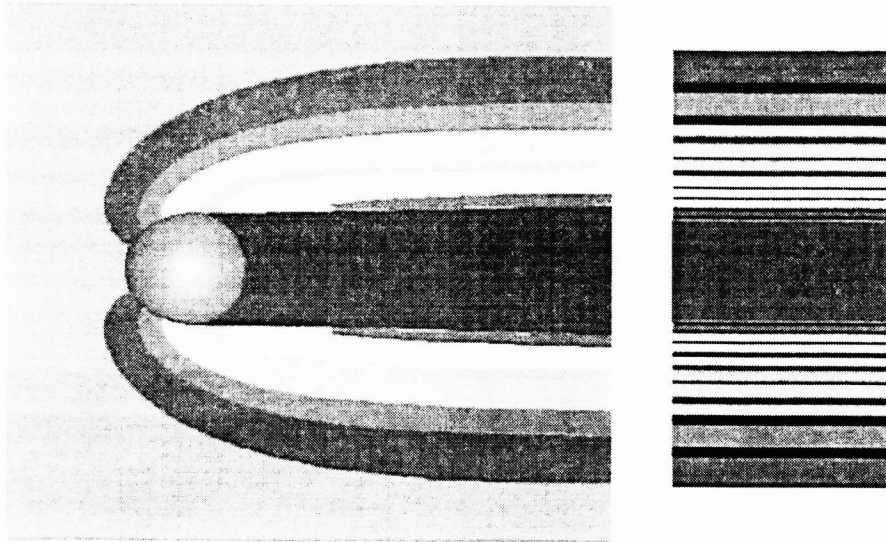


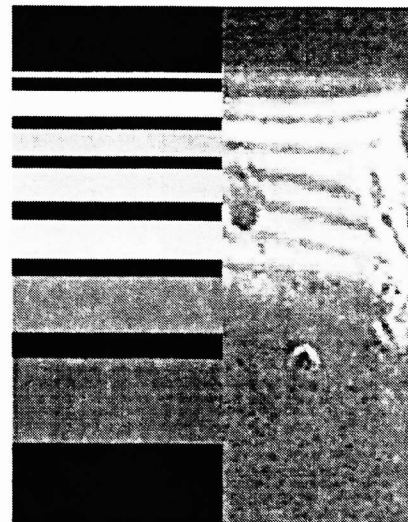
Figure 10: Ray-trace along a hot cylinder. left: side view in plane of tracing.
right: simulated 'Schlieren' image in image plane.

Figure 10 shows how individual rays trace through the temperature gradient. Each ray is assigned a color depending on the angle between the ray and the optical axis at that particular position in space. If a ray would continue from that point without further interference, it would intersect with that color on the filter. This way the 'evolution' of the angular distribution of rays going through the temperature gradient can be followed. It shows at what point the strongest deflection takes place. The picture on the right shows the simulated 'Schlieren' image calculated at the image plane.

5.2 Comparison of ray-traced and 'real' Schlieren images

Figure 11 shows a close-up comparison of the calculated (left) and 'real' Schlieren image of the temperature profile along side the hot cylinder. Although there is resemblance, the images are not equal as would be expected if the ray-tracing simulation was correctly.

Figure 11:
Comparison between calculated (left)
and 'real' schlieren image (right)



Having established that the ray-trace program itself works correctly for a index gradient lens, the inconsistency should be ascribed to the input data. The appearance of the calculated Schlieren image is determined by two functions: (1) the assumed (measured) temperature gradient and (2) the refractive index of water in relation to the temperature.

It is possible that the temperature profile function was not completely accurate. The measurement could have been influenced by some artifacts. The thermocouple and the supporting needle could have acted as a heat sink, lowering the temperature measured. Furthermore, the temperature measured could be lower due to convection above the cylinder surface and around

the thermocouple. Still, the error in the temperature measurement is estimated not to be larger than 3 degrees. This does not account for the difference between the calculated and the measured images. By increasing the entire temperature profile in Figure 9, to compensate for the artifacts discussed, the calculated 'Schlieren' image does still not match the 'real' image as shown in Figure 13 left and middle panel.

For this experiment, the assumption was made that the refractive index function of the gel, in which the cylinder was embedded, was equal to water. This assumption was in first instance legitimate since the gel consisted for 90% of water. It can be expected that the refractive index of the gel is slightly higher than water due to the higher density of the gel. However, a constant increase of the refractive index function has little effect on the calculated Schlieren images. On the other hand, if the refractive index dependence of the gel on the temperature would slightly differ from the dependence of water, the effect could be significant. Figure 12 shows an estimated relation for the refractive index of the gel in relation to temperature.

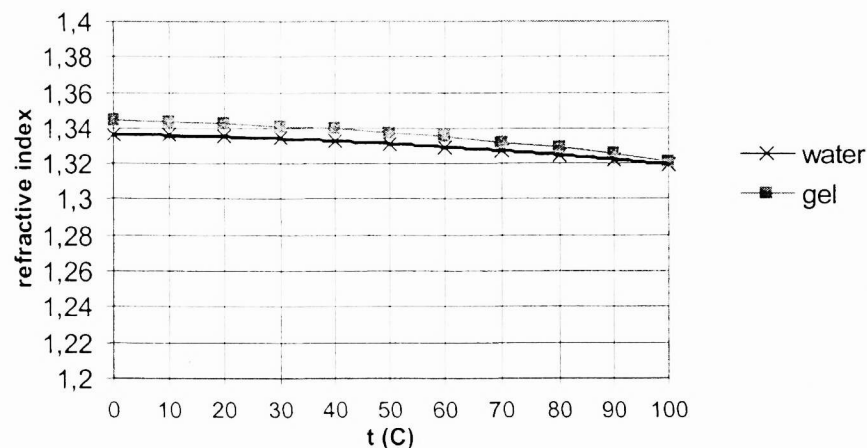
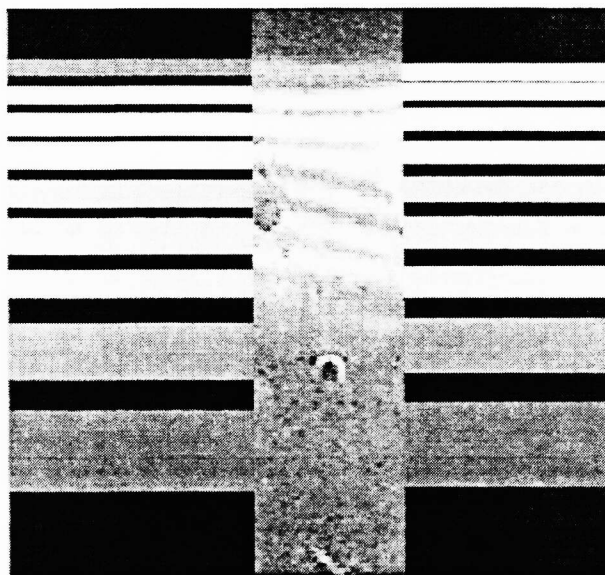


Figure 12: Potential variance between the refractive index of water and gel in relation to temperature

The estimated curve for the gel is assumed to be slightly steeper in the higher temperature region. The largest difference (at 0 °C) is only 0.6 percent. When this relation is used as input for the ray-trace program, the calculated Schlieren image changes considerably compared to the original situation. The refractive index 'corrected' image shows to be more consistent with the 'real' Schlieren image (Figure 13, right and middle panel, respectively).

Figure 13:
Comparison between
the 'temperature corrected' image (left),
the 'real' image (middle) and
the 'refractive index corrected' image (right).



This does not necessarily mean that the relation of the refractive index to temperature for gel assumed in Figure 12 is correct. It just demonstrates how influential the refractive index function is on the resulting calculation. The difference between the calculated and the actual images is most likely caused by a combination of factors discussed.

5.3 Improvements of the Schlieren ray-trace simulation

It should be clear from the previous discussion that knowledge of the relation of the refractive index of the gel in relation to the temperature is essential. This would contribute to the accuracy of the 'Schlieren' images generated with the trace program. As to the ray-trace program itself, the program can be made more user friendly for 'on-line' changing of parameters and conversion of data to image files. The speed and accuracy of the program could be improved significantly by the introduction of an active feedback on size of the iteration steps. When tracing through a steep gradient, the iteration steps should be small while large steps could be taken when the ray is away from the temperature gradient. With a small program loop this situation could be tested and the size of the iteration steps could be determined before doing the calculation. At present, the Schlieren ray-trace program works the 'wrong way' around; first a temperature profile has to be defined, and then the program generates the Schlieren image. Ideally, the program should calculate a temperature distribution from a 'real' Schlieren image in combination with some information on the geometry of the temperature gradient. The program would then act as a kind of mathematical solver. However, it will be difficult to accomplish and will need at least a mainframe computer. Still assumptions have to be made regarding the temperature distribution to ensure a converging solution.

6. CONCLUSIONS

The ray-trace program developed in this study has proven to be a helpful tool to help interpretation of color Schlieren images from simple geometries as to absolute temperatures. Expanding the code might enable the quantification of temperature gradients. Such information is valuable for the clinical application of energy source such as lasers.

7. REFERENCES

1. Verdaasdonk R.M., Borst C., 'Optical technique for color imaging of temperature gradients in physiological media: a method to study thermal effects of CW and pulsed lasers', in Laser Tissue Interaction IV, S.L. Jaques (ed), Vol.1882, pp.355-366, SPIE, Bellingham, 1993
2. Swol, C.F.P.v., Verdaasdonk, R.M., Vliet, R.J.v., Molenaar, D.G. and Boon, T.A. Side-firing devices for laser prostatectomy. World Journal of Urology 13:88-93, 1995.
3. Grimbergen, M.C.M., Verdaasdonk, R.M. and Swol, C.F.P.v. Correlation of thermal and mechanical effects of the holmium laser for various clinical applications. SPIE proceedings 3254:69-79, 1998.
4. Verdaasdonk, R.M., Sachinopoulou, A., Grundeman, P.F. and Beek, J.F. Working mechanism of pulsed CO₂, Holmium and Excimer laser systems in view of Trans-Myocardial Revascularization (TMR): in vivo implications. In: TMLR Management of coronary artery diseases, edited by Klein, M., Schulte, H.D. and Gams, E. Berlin: Springer-Verlag, p. 143-151, 1998.
5. Swol, C.F.P.v., Vliet, R.J.v., Grimbergen, M.C.M. and Verdaasdonk, R.M. Tissue effects of argon gas flow during electrosurgery. SPIE proceedings 3249:68-71, 1998.
6. Verdaasdonk, R.M. Imaging laser induced thermal fields and effects. In: Laser-Tissue interaction VI, edited by Jacques, S.L. Bellingham: SPIE Proceedings 2391, , p. 165-175, 1995.
7. Howes, W.L. Rainbow schlieren and its applications. Appl Optics 23:2449-2460, 1984.
8. Settles, G.S. Color Schlieren Optics - A review of techniques and applications. In: Flow Visualization, Vol.2, edited by Merzkirch, W. New York: Hemisphere, p. 749-759, 1982.
9. Giancoli, Physics for scientists and engineers. Prentice hall international editions.1988.
10. Hecht, E. and Zajak, A. Optics, Reading,MA:Addison-Wesley, pp. 478-481, 1979.
11. H.Friberg,A.J.Insel & L.E.Spence, Linear algebra, Prentice Hall.1989.
12. Weast, RC ed. CRC Handbook of Chemistry and Physics. Boca Raton, Florida: CRC Press, 1984.